A 12.5-Gb/s Fresnel Zone Coupled Fully Rotatable 60-GHz Contactless Connector in 65-nm CMOS Process

Hossein Zaheri, Walter Wargacki, Caleb Romero, Yanghyo Kim
Stevens Institute of Technology, USA

***Abstract* — This work presents a 60-GHz contactless connector that can fully rotate without physical contact. Conventional connectors suffer poor mechanical reliability, maneuverability, and signal integrity when handling moving or rotating parts, such as in robotic arms, often becoming bottlenecks in high-precision autonomous systems. Our implemented system consists of a 60-GHz CMOS transmitter (Tx), receiver (Rx), and compact antenna to enable fully rotatable and energy-efficient contactless connector solutions. Two folded-dipole antennas communicate in a radiative Fresnel zone, where both longitudinal and transversal electromagnetic fields propagate simultaneously. We exploit the longitudinal electric field component to de-sensitize the polarization mismatch over the entire rotational angle. In addition, we employ an automatic gain control (AGC) loop and offset canceling amplifiers to compensate for the transmission characteristic degradation and signal imbalance when connectors rotate. The demonstrated system consumes 56 mW of power under a 1-V supply while transferring 12.5-Gb/s of data rate, achieving 4.5-pJ/bit energy efficiency.**

***Keywords*—CMOS, Contactless Connector, Millimeter-Wave, OOK Modulation, Non-Coherent Detection, Radiative Fresnel Zone, Rotational Connector.**

I. Introduction

Conventional electrical connectors often determine a device's form factor, maneuverability, lifespan, and communication bandwidth because of the physical constraints between connecting components. We especially face more deteriorated signal integrity issues when connectors must move or rotate for greater flexibility. In addition, the demand for larger bandwidth continues increasing when connectors support autonomous systems, such as industrial robotic systems. For instance, highly sophisticated autonomous robots require high-definition camera sub-systems with multi-Gb/s bandwidth as they rely on deep learning-enabled machine vision and edge computing technologies [1]. Mechanically rotatable connectors adopted in today's commercial and industrial applications provide less than 1-Gb/s data rate, imposing serious bandwidth scalability challenges [2]. Recent advances in non-contact rotatable connectors realized up to 6-Gb/s data rate by magnetically coupling baseband pulses between inductors or transmission line couplers at a few mm distances, but ultimately, they still meet the difficulties in bandwidth scalability [3]-[6]. Antenna-coupled millimeter-wave contactless connectors demonstrated bandwidth scalability, but none proved the tolerance when connectors rotate [7]-[9].

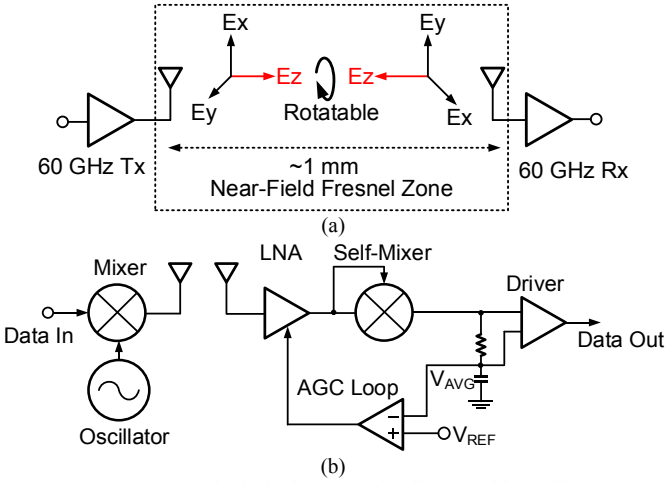

Figure 1. (a) Conceptual block diagram of fully rotatable millimeter-wave wireless interconnect in radiative Fresnel zone, and (b) block diagrams of the implemented transmitter and receiver in 65-nm CMOS process.

In this work, we designed a 60-GHz CMOS transmitter (Tx) and receiver (Rx) and demonstrated a fully rotatable contactless connector operating at a 12.5-Gb/s data rate. As shown in Fig. 1(a), we place the Tx and Rx antennas in a radiative Fresnel zone, where both transversal and longitudinal electromagnetic fields propagate simultaneously (i.e., we exploit the longitudinal fields' polarization insensitiveness to rotate the Tx and Rx antennas continuously). We can readily define the Fresnel zone to specify our contactless connector's operating distances according to (1).

$$0.62\sqrt{\frac{D^3}{\lambda}} < R < \frac{2D^2}{\lambda} \quad (1)$$

D: Antenna dimension
R: Distance between the two antennas
λ: Wavelength at operating frequency

Based on the optimized 1.8-mm antenna dimension (shown in Fig. 2(a)) and the operating frequency of 60-GHz, in theory, our system can sustain the displacement between 0.6-mm and 1.3-mm while either the Tx or Rx rotates. We implemented a non-coherent on-off-keying (OOK) Tx/Rx to minimize the system complexity, as shown in Fig. 1(b). The Tx consists of a 60-GHz free-running oscillator and upconverting mixer, and the Rx starts with a two-stage low-noise amplifier (LNA) and down-converts modulated signals to the baseband by a self-mixer. Although we reduce the polarization sensitivity by

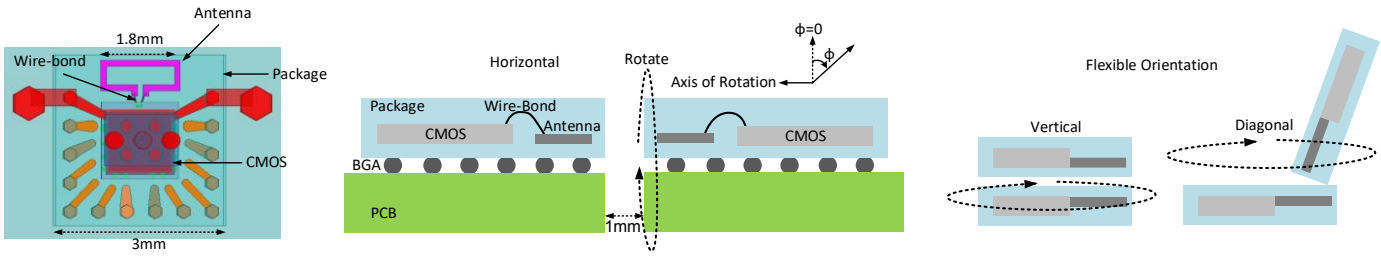

(a) (b) (c)

Fig. 2. (a) 60-GHz antenna model designed in HFSS software, (b) block diagram of side-launched two antennas that can rotate, and (c) additionally feasible launching positions.

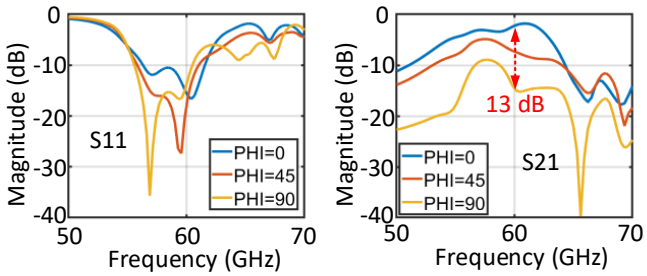

Fig. 3. Simulated S11 and S21 at rotation angles of 0, 45, and 90 with horizontal Tx/Rx placement.

arranging antennas in the radiating Fresnel zone, the antennas still suffer transmission characteristic variations because of the misalignment. We implemented an automatic gain control (AGC) loop to overcome such variations by comparing the average value of the self-mixer output to the target reference voltage set by the desired signal strength. Additionally, we implemented a DC offset cancellation loop in the driver stage to correct the signal imbalance when converting single-ended signals to differential signals at the self-mixer output. The proposed AGC will play a critical role when further scaling the communication bandwidth by multi-level signaling.

II. 60-GHz Antenna Coupler Design

We designed a folded-dipole antenna in a standard package to miniaturize our connector size and enable a robust assembly, as shown in Fig. 2(a). We connect the 60-GHz CMOS Tx/Rx and antennas inside the package using wire bonds. We then interconnect the rest of the CMOS input/output to a printed circuit board using re-distribution layers (RDL) and ball grid arrays (BGA). Unlike the inductor or transmission line couplers, our millimeter-wave contactless connectors offer much greater flexibility in placement orientation because of omnidirectional field propagation in the radiative Fresnel zone. For instance, we can not only place the Tx and Rx horizontally but also we can place them vertically or diagonally, as illustrated in Fig. 2(b) and (c). We simulated the return loss (S11) and transmission characteristics (S21) of horizontally coupled contactless connectors to study the rotational effects using HFSS software. As shown in Fig. 3(a), the S11 maintains better than -10 dB between 0 and 90 degrees. In Fig. 3(b), the S21 changes 13 dB at the 60-GHz operating frequency when one connector turns 90 degrees.

III. 60-GHz CMOS Transmitter and Receiver

We fully integrate the Tx and Rx in a single chip using a half-duplex transformer (i.e., only one path turns on for each Tx and Rx mode), as shown in Fig. 4(a). The front-end transformer provides a matching condition for both Tx and Rx. In the Tx, a free-running oscillator generates 60-GHz carrier signals and drives the up-conversion mixer's differential pair. We isolate the DC bias conditions between the oscillator and mixer using a transformer to optimize the Tx energy efficiency. The Tx generates a 0 dBm output power without an additional driver stage.

We implement a two-stage common source LNA with cascode devices providing a 20-dB gain and a non-coherently down-converting self-mixer in the Rx front-end. Because of their superior stability and DC isolation capabilities, we cascade them using compact transformers between the LNA and self-mixer stages. After the LNA, a self-mixer down-converts carrier-modulated signals to the baseband signals without carrier synchronization circuits. We also create an average DC value of the demodulated signals via an RC filter for automatic gain control. Note that the self-mixer generates a lower average value when it receives a higher input swing because of the higher demodulated currents flowing into the common drain node.

We can ensure the AGC settles to the reference voltage using the above self-mixer property. As shown in Fig. 4(b), assume the average DC value begins lower than the reference and gradually tracks the reference voltage (i.e., the self-mixer's input swing is initially higher than our desired amplitude). A slight increase in the average DC value (if it tracks the reference correctly) reduces the output of an operational amplifier (OPAMP) and consequently decreases the self-mixer's input swing (due to the reduced LNA gain). The reduced self-mixer input swing increases the average DC value and continues until it converges in the AGC loop. We also utilize the average DC value to convert the single-ended signals after the down-conversion to differential signals in the high-speed driver stage. However, the differential conversion suffers a signal imbalance and DC offset. As shown in Fig.

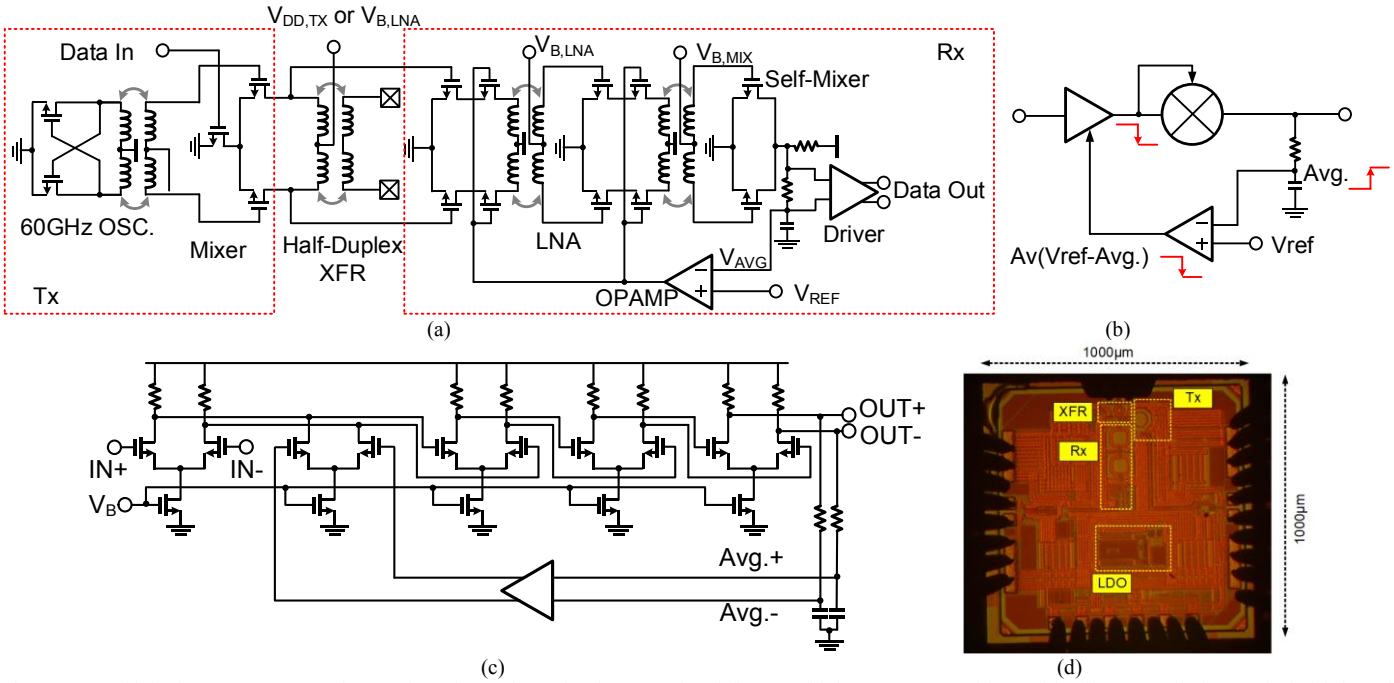

Fig. 4. (a) Half-duplex 60-GHz transmitter and receiver schematic, (b) AGC signal flow, (c) high-speed output driver with offset cancellation, and (d) fabricated half-duplex Tx/Rx in 65-nm CMOS process.

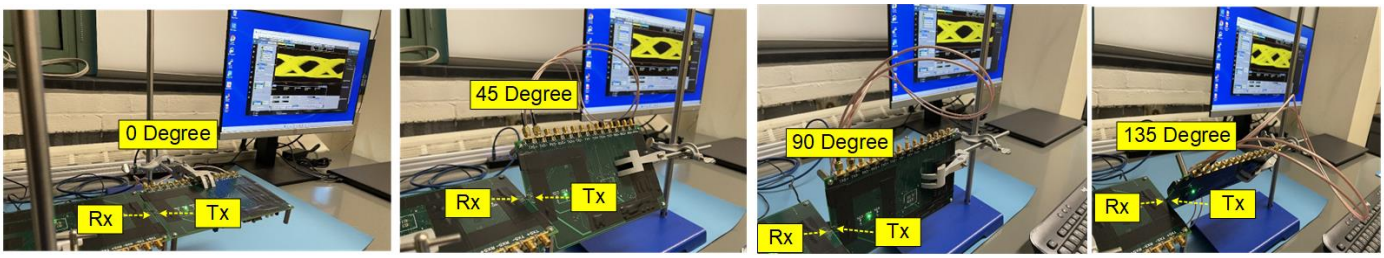

Fig. 5. Measurement setup with rotation angles of 0, 45, 90, and 135 degrees.

Fig. 6. (a) Measured eye diagrams at 10-Gb/s, and (b) measured eye diagrams at 12.5-Gb/s.

4(c), we extract the DC average values of the driver's output signals and feed them to the current subtractor at the driver's first stage. If the average value of the positive output signal is higher than the negative signal, we subtract more DC currents at the negative signal chain to raise the output common-mode level relative to the positive signal chain. We fabricated the Tx/Rx in a 65-nm CMOS process, as shown in Fig. 4(d).

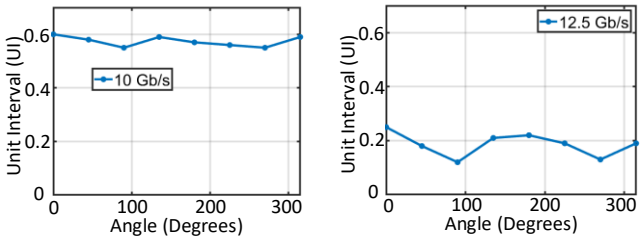

Fig 7 Measured unit intervals over 360 degree rotational angles

Table 1. Comparison between rotational contactless connectors.

	[3] ISSCC'13	[4] ISSCC'13	[5] IMS'21	[6] JSSC'22	This Work
Data Rate (Gb/s)	1.2	5.5	2.6	6	12.5
BER	$<10^{-12}$	$<10^{-12}$	$<10^{-12}$	$<10^{-12}$	$<10^{-12}$
Energy Efficiency (pJ/b)	3.9	36	20	9.8	4.5
Coupler Size (mm^2)	5.8	144	N/A	49	3.2
Distance (mm)	1	5	0.5	3	1
pJ/b/mm	3.9	7.2	40	3.3	4.5
Coupler	Inductive	Inductive	Split-Ring Rosonator	Transmission Line	Antenna
Carrier	Baseband	Baseband	16 GHz	Baseband	60 GHz
Technology	130nm CMOS	180nm CMOS	65nm CMOS	40nm CMOS	65nm CMOS

IV. Measurement Results

We captured the measurement setup of the rotatable contactless connector in Fig. 5. For the proof of concept, we placed the Tx and Rx in the horizontal orientation at a 1 mm distance. As shown in Fig. 6(a), we can transfer 10-Gb/s data streams at any rotational angle while maintaining the same amplitude and nearly equal unit intervals. Based on the estimated signal-to-noise ratio from the eye-diagram, which is higher than 20 dB, we achieved better than 10^{-12} bit error rate (BER) for all rotational angles. In Fig. 6(b), we transmitted a maximum data rate of 12.5-Gb/s with acceptable unit intervals. The estimated BER is better than 10^{-7} in the worst case. We summarized the unit intervals at each rotational angle at 10-Gb/s and 12.5-Gb/s, respectively, as shown in Fig. 7. Finally, we compared our work with previously introduced rotatable contactless connectors in Table 1. We achieved approximately twice the higher data rate and energy efficiency and nearly ten times smaller coupler size compared to the state-of-the-art transmission line couplers in [4].

V. Conclusion

We presented a rotatable contactless connector using 60-GHz Tx/Rx and antennas in this work. We placed two antennas in a radiating Fresnel zone to reduce the polarization sensitivity. We designed an automatic gain control loop and offset cancellation loop to achieve nearly the same unit intervals at any rotational angles. We demonstrated the maximum data rate of 12.5-Gb/s while consuming 56-mW under a 1-V supply.

Acknowledgement

This work was sponsored by the DARPA YFA program.

References

[1] A. Zeng, *et al.*, "Multi-view self-supervised deep learning for 6D pose estimation in the Amazon picking challenge," *Proc. IEEE Int. Conf. Robot. Automat.*, May 2017.

[2] G. Dorsey and M. Harris, "Avoiding data bottlenecks in rotating systems – copper or fiber," *Moog Inc., Elma, NY, USA, White Paper,* Mar. 2020.

[3] H. Cho, *et al.*, "A 1.2 Gb/s 3.9 pJ/b mono-phase pulse-modulation inductive-coupling transceiver for mm-range board-to-board communication," *IEEE Int. Solid-State Circuits Conf. (ISSCC)*, 2013.

[4] K. Hijioka, M. Matsudaira, K. Yamaguchi, and M. Mizuno, "A 5.5 Gb/s 5 mm contactless interface containing a 50 Mb/s bidirectional sub-channel employing common-mode OOK signaling," *IEEE Int. Solid-State Circuits Conf. (ISSCC)*, 2013.

[5] G. Schuppener, et al., "A multi-Gbps, energy efficient, contactless data-communication link for machine-to-machine (M2M) interaction with rotational freedom," *IEEE MTT-S Int. Microw. Symp. Dig.*, 2021.

[6] A. Kosuge, M. Hamada, and T. Kuroda, "A 6-Gb/s inductively-powered non-contact connector with rotatable transmission line coupler and interface bridge IC," *IEEE J. Solid-State Circuits,* vol. 57, no. 2, pp. 535-545, 2022.

[7] K. Kawasaki, *et al.*, "A Millimeter-Wave Intra-Connect Solution," *IEEE J. Solid-State Circuits,* vol. 45, no. 12, pp. 2655-2664, 2010.

[8] Y. Kim, *et al.*, "A millimeter-wave CMOS transceiver with digitally pre-distorted PAM-4 modulation for contactless communications," *IEEE J. Solid-State Circuits*, vol. 54, no. 6, pp. 1600-1612, Jun. 2019.

[9] Y. Kim, S.W. Tam, and F. Chang, "Millimeter-wave contactless connectors: from fundamental research to commercialization," *IEEE Microw.*, vol. 23, no. 4, 2022.